ARTICLE

OBC
www.rsc.org/obc

Design, synthesis, biological activity and structural analysis of cyclic peptide inhibitors targeting the substrate recruitment site of cyclin-dependent kinase complexes

Martin J. I. Andrews, Campbell McInnes, George Kontopidis, Lorraine Innes, Angela Cowan, Andy Plater and Peter M. Fischer

Cyclacel Limited, James Lindsay Place, Dundee, Scotland, UK DD1 5JJ.
E-mail: mandrews@cyclacel.com; Fax: +44 1382 206067; Tel: +44 1382 206062

Received 16th June 2004, Accepted 13th August 2004
First published as an Advance Article on the web 9th September 2004

Inhibition of cyclin A- and cyclin E-associated cyclin-dependent kinase-2 (CDK2) activities is an effective way of selective induction of apoptotic cell death *via* the E2F pathway in tumour cells. The cyclin groove recognition motif (CRM) in the natural CDK-inhibitory (CDKI) tumour suppressor protein $p27^{KIP1}$ was used as the basis for the design and synthesis of a series of cyclic peptides whose biological activity and structural characterisation by NMR and X-ray crystallography is reported. Whereas linear $p27^{KIP1}$ sequence peptides were comparatively ineffective, introduction of side chain-to-tail constraints was found to be productive. An optimal macrocyclic ring size for the conformational constraint was determined, mimicking the intramolecular H-bonding system of p27. Molecular dynamics calculations of various macrocycles suggested a close correlation between ring flexibility and biological activity. Truncated inhibitor peptide analogues also confirmed the hypothesis that introduction of a cyclic conformational constraint is favourable in terms of affinity and potency. The structural basis for the potency increase in cyclic *versus* linear peptides was demonstrated through the determination and interpretation of X-ray crystal structures of complexes between CDK2/cylin A (CDK2A) and a constrained pentapeptide.

Introduction

The CDK2A kinase complex is required for cell cycle progression through S phase, where DNA is replicated in preparation for mitosis and cytokinesis in proliferating cells.[1] The CDK2 subunit requires complexation and activation loop phosphorylation before a fully active CDK2A complex is obtained.[2] Levels of cyclin A vary during the cell cycle, causing appropriate up- and down-regulation of transcriptional promoters (E2F family) and repressors (retinoblastoma protein (pRb)-like proteins).[3] In this way proliferating cells are able to control entry and exit from S phase, thus ensuring the single complete cycle of DNA replication necessary for maintenance of genomic integrity. The central role of CDK2A has made this kinase of interest as a potential target for intervention in proliferative diseases such as cancer.[4] Pharmacological inhibition of CDK2 was shown to induce G1/S cell cycle arrest through maintaining pRb hypophosphorylation in G1, and to promote programmed cell death through apoptosis by blocking E2F1 phosphorylation in S phase.[5]

A large number of proteins interact with CDK2A, both as substrates for phosphorylation and as inhibitors.[6] Amongst the latter the CDKIs including $p21^{WAF1}$ and $p27^{KIP1}$ play important roles in CDK2A regulation. Certain CDK2A substrates, *e.g.* histone H1, are phosphorylated directly, but many others react in a two-step process of initial recognition by cyclin A, followed by phosphorylation by the kinase subunit. This class of substrates includes both the pRb and E2F protein families. Initial recognition by cyclin A presumably positions the substrate for effective phosphorylation by CDK2, and a series of fusion peptides showed that phosphorylation critically depends on the presence of a cyclin A recognition motif.[7]

The binding site on cyclin A is termed the cyclin binding groove (CBG) and is formed by a shallow hydrophobic surface cleft.[8] Those proteins known to bind *via* the CBG share a level of homology, of the general form (termed the cyclin recognition motif (CRM)) Arg-Xaa-Leu-Yaa-Zaa, where Xaa is any residue and one of Yaa and Zaa is a hydrophobic residue, usually Phe.[6] A crystallographic structure of a CDK2A-$p27^{KIP1}$ protein complex has been reported,[9] showing that the conserved Arg in the CRM (Arg-Asn-Leu-Phe-Gly in the case of $p27^{KIP1}$) makes water-mediated contacts with acidic surface residues of cyclin A, while the Leu and Phe residues make a number of contacts with Met^{210}, Ile^{213}, and Leu^{253}, which form the hydrophobic pocket of the CBG. Additionally, intramolecular H-bonding interactions can be observed between the Asn and Gly residues in the $p27^{KIP1}$ CRM (Fig. 1).

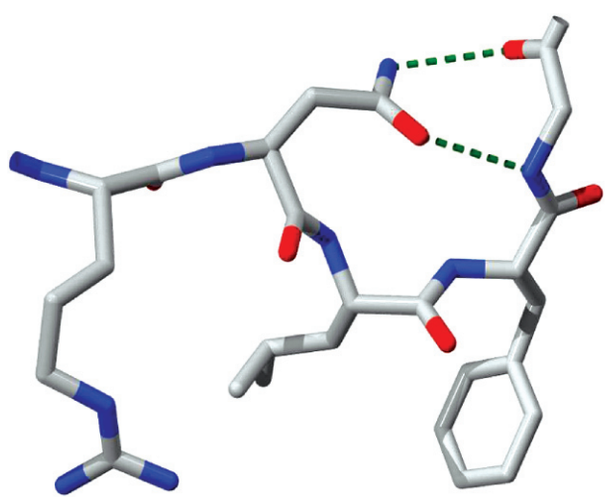

Fig. 1 Conformation of the Arg-Asn-Leu-Phe-Gly CRM present in the crystal structure of the CDK2A-$p27^{KIP1}$ complex. The intramolecular H-bonds between the Asn side chain and the Gly backbone are indicated with broken lines.

This observation motivated us to design synthetic peptide **5** containing side chain-to-tail cyclic constraints. Incorporation of structural constraints is a well-established method for improving potency in compounds, as increasing conformational rigidity results in a lower entropic cost for binding.[10]

Several solid-phase and solution strategies allow the assembly of head-to-tail and side chain-to-tail cyclic peptides.[11] In the case of solid-phase peptide synthesis, these include the use of differential protecting groups allowing on-resin cyclisation followed by separate cleavage, and the synthesis of protected

DOI: 10.1039/b409157d

peptide fragments that can be cyclised after cleavage from the solid support. The idea of using cyclisation as a method of cleavage from the solid support has also been developed, using both oxime and sulfonamide resins.[12–14] It was this latter strategy that we decided to use, employing the Ellman "safety catch" linker (Scheme 1). In alternatives such as the oxime resin method, the linker is permanently activated to nucleophilic attack, and slow cleavage is also seen during the required repetitive acidolytic Boc deprotection steps. The Ellman linker can be loaded using standard methods, and whilst in the unactivated form it is stable to standard Fmoc strategy deprotection and coupling conditions, and it can subsequently be activated for nucleophilic cleavage.[15] This occurs by alkylation of the sulfonamide nitrogen, rendering the sulfonamide carbonyl susceptible to nucleophilic attack. Such cleavage is normally achieved with external nucleophiles, however use of an internal amine nucleophile to give an intramolecular reaction is also possible. This approach has recently been used for the generation of head-to-tail cyclic peptides.[14]

Results and discussion

Structure-guided design of cyclic peptides

In previous studies we defined extensively the structure–activity relationships of the $p21^{WAF1}$ CRM Arg-Arg-Leu-Ile-Phe.[6,16,17] We found that for optimal presentation of the critical *Phe* and *Leu* side chains, the $p21^{WAF1}$ sub-motif *Leu*-Ile-*Phe*-NH_2 gave more favourable conformations in comparison to the $p27^{KIP1}$ *Leu*-*Phe*-Gly-NH_2 sub-motif. Peptides incorporating the former sub-motif were found to be significantly more potent CDK2A inhibitors than those containing the latter. Inspection of the CDK2A/$p27^{KIP1}$ complex crystal structure reveals intramolecular H-bonds between the Asn side chain amide and the Gly in the CRM, presenting the *Phe* and *Gly* side chains in a specific conformation (Fig. 1). This observation led to the idea that incorporation of a covalent cyclic constraint mimicking this intramolecular H-bond might lead to an increase in the binding affinity of peptides with the Leu-Phe-Gly sub-motif.

Modelling studies were undertaken to determine the most effective method of incorporating a cyclic constraint into synthetic peptide inhibitors with the Asn-*Leu*-*Phe*-Gly sub-motif. The initial hypothesis employed Lys in place of Asn, and an amide bond from the Lys ε-NH_2 to the Gly carboxyl. This constraint was modelled through energy minimization, keeping the critical Leu and Phe side chains in appropriate positions. It was found that this design matched the observed complex structure (Fig. 1) closely and thus represented a basis for the synthesis of the side chain-to-tail cyclic structure.

Different ring sizes were then modelled, incorporating various diamino acid residues other than Lys, including 2,3-diaminopropionic acid (A_2pr), 2,4-diaminobutanoic acid (A_2bu), and ornithine (Orn), *i.e.* n = 1, 2, or 3 in **5** (Scheme 1). The cyclic structures were energy-minimized and molecular dynamics simulations were performed in order to explore the conformational space accessible for each peptide. It was found that the RMS difference between the average of all frames of the molecular dynamics trajectory and the $p27^{KIP1}$ crystal structure coordinates was at a minimum for the Lys- (n = 4 in **5**) and maximal for the A_2bu-cyclised peptide.

Synthesis of side chain-to-tail cyclic peptides

We initially used the $p21^{WAF1}$ CRM His-Ala-Lys-Arg-*Arg*-*Leu*-*Ile*-*Phe*[16] for our design, into which the *Xaa*-*Leu*-*Phe*-*Gly* (Xaa: diamino acid) system was substituted (*i.e.* **5**, **Seq** = H-His-Ala-Lys-Arg-). Boc-His(Boc) was incorporated as the *N*-terminal residue in precursors **3** and **4**, so the free peptides could be revealed using a single final acidolytic deprotection step.

Loading and peptide synthesis on the sulfamylbutyryl resin **1** was performed by literature methods.[15] Glycine was incorporated in acceptable yields to give (**2**) by quantitative Fmoc test (0.3 mmol g^{-1}). Although the loading obtained was lower than reported in the literature, we reasoned that the low loading would be beneficial for our approach, as the pseudo-dilution effect obtained on solid phase should decrease oligomer formation.[18] The peptides (**3**) were then assembled by standard Fmoc methodology.[19] In each case, the amide bridge residue was incorporated as the 4-methyltrityl (Mtt)-protected side-chain derivative, allowing selective mild acid cleavage prior to cyclisation.[20] The first steps in this process were the standard sulfonamide *N*-alkylation of resins (**3**) with iodoacetonitrile, followed by Mtt cleavage using dilute TFA. A short treatment time was used to reduce the level of concomitant resin cleavage.

The reported standard conditions for the nucleophilic cleavage of sulfonamide linker **4** is by means of simple incubation of the resin with external nucleophiles in THF at room temperature. These conditions were attempted, but were found to be ineffective for the required intramolecular formation of the desired macrolactams (**5**). Although cyclisation did appear accelerated at higher temperatures, THF was not found to be a suitable solvent due to the insolubility of the cyclised products. Various

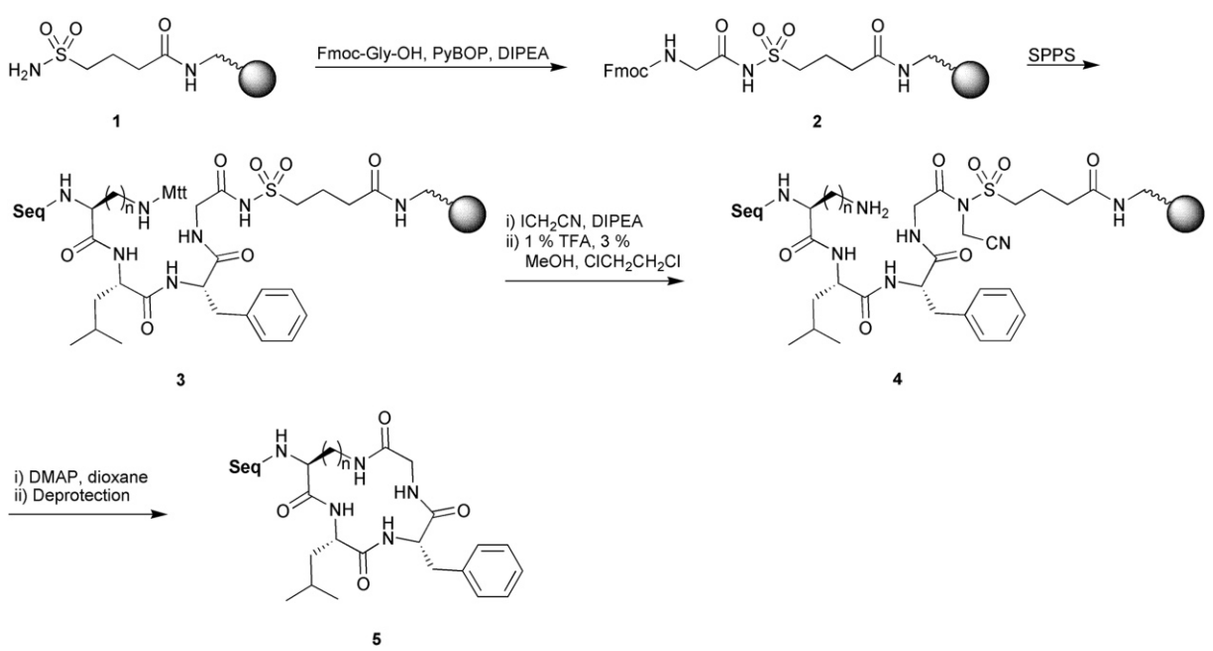

Scheme 1

Table 1 Peptide structure–activity relationships

	Structure					
	Seq-*Xaa*-Leu-Phe-Gly—		Inhibition (IC_{50}/μM)			
Peptide no.	**Seq**	*Xaa*	Competitive cyclin A binding assay[a]	S.D.	CDK2A-pRb kinase assay[b]	S.D.
5a	Ac-Ala-Ala-Abu-Arg	Lys	0.63	0.09	0.53	0.12
5b	Ac-Ala-Ala-Abu-Arg	Orn	50.0	5.46	24.4	7.21
5c	Ac-Ala-Ala-Abu-Arg	A_2bu	>250		123.7	18.3
5d	Ac-Ala-Ala-Abu-Arg	A_2pr	>250		>250	
5f	Ac-Arg	Lys	19.2	0.67	22.3	0.31
5e	Ac-Ser-Ala-Abu-Arg	Lys	2.25	0.04	1.52	0.17
5g	H-His-Ala-Lys-Arg	Lys	0.36	0.12	2.65	1.04
6	Ac-Ala-Ala-Abu-Arg-Asn-Leu-Phe-Gly-NH_2		59.4	8.26	49.2	37.4
7	Ala-Abu-Arg-Asn-Leu-Phe-Gly-NH_2		24.5	4.95	35.5	4.95
8	Abu-Arg-Asn-Leu-Phe-Gly-NH_2		>50		>100	
9	Arg-Asn-Leu-Phe-Gly-NH_2		>50		>100	

[a] Fluorescence polarization assay using the ligand fluoresceinyl-Ahx-His-Ala-Lys-Arg-Arg-Leu-Ile-Phe-NH_2. [b] Incorporation of ^{32}P from ATP (total [ATP] = 0.1 mM) into pRb substrate.

alternative solvents were then evaluated to identify the most appropriate for the reaction. Standard peptide synthesis solvents such as DMF and DCM were found to be ineffective, as the former gave contamination with by-products, and the latter only low yields of the desired product. This was thought to be due to the low temperature attainable with refluxing DCM giving insufficient energy for cyclisation, however the higher boiling dichloroethane was also ineffective. 1,4-Dioxane was found to be the most effective, and heating the peptidyl resins **4** at 80 °C overnight in this solvent led to the best recovery of the desired macrolactams (**5**).

Despite optimisation, low yields were obtained with products found to contain both open chain and head-to-tail cyclised peptides, due to competing processes in the synthetic route. A recent kinetic investigation of the *N*-Mtt cleavage reaction has been perfomed.[21] This work suggests that the kinetics of cleavage are slower than previously thought, in turn suggesting longer deprotection times are required. Short cleavage times were used in the synthesis, in order to reduce potential cleavage of the α-amino and side chain Boc protecting groups, which could result in cross-reaction. Incomplete Mtt removal prior to cyclisation may thus explain the levels of open-chain peptides recovered. The formation of head-to-tail products requires free α-amino group, possibly due to thermolytic cleavage of the α-*N*-Boc group during the cyclisation reaction. This would generate a second, competing nucleophile and hence a second product.

Attempts were then made to reduce these problems by use of a simplified peptide sequence. In the course of our peptide structure–activity studies we had identified an optimised $p21^{WAF1}$ CRM (Ala-Ala-Abu-Arg-Ser-*Leu-Ile-Phe* (Abu: 2-aminobutyric acid)).[6] We therefore applied the *Xaa-Leu-Phe-Gly* system in this context, with *N*-terminal acetylation (*i.e.* **5**, **Seq** = Ac-Ala-Ala-Abu-Arg-), which blocked the potential formation of the head-to-tail product. This approach was more effective, affording the desired compounds (with n = 1–4) cleanly. Indeed, although levels of open chain product were also recovered, no head to tail form was identified.

Macrocyclic lactam formation reactions are generally quite low yielding, regardless of the method used. The yields from SPPS of open chain peptides can also be low, dependent on sequence, and in the case of the open chain analogue of the sequence used (*i.e.* peptide **6**) a yield of 25% after purification (calculated from resin loading) was obtained. In comparison, the yields obtained for the cyclic peptides were in the range 1–5% after HPLC purification (Table 3). The difficulty inherent in the formation of macrocyclic lactams can clearly be seen in the yields. Solution methods additionally suffer from the generation of oligomeric products, even under the normal high dilution conditions used. In the current method, oligomer formation is not observed, giving simplified purification.

Biological activity of cyclic peptides

The linear peptides based on the $p21^{WAF1}$-derived CRM sub-motif Leu-Ile-Phe, in both the native and optimised *N*-terminal contexts are highly potent inhibitors of CDK2A enzymatic activity on substrates dependent on initial cyclin A recognition. In contrast, linear peptides containing the $p27^{KIP1}$-derived CRM sub-motif Leu-Phe-Gly, regardless of *N*-terminal extension, are far less potent,[6] *e.g.* the linear control peptide **6** (Table 1), and potency decreases rapidly as the peptide is truncated from the *N*-terminus (**7**–**9**).

Introduction of the Lys-to-Gly constraint into the optimised CRM *N*-terminal sequence, *i.e.* peptide **5a**, led to a remarkable potency increase of two orders of magnitude. Similarly, this constraint was also productive in the $p27^{KIP1}$- (peptide **5e**; isosteric Abu in place of Cys) and original $p21^{WAF1}$ *N*-terminal sequences (peptide **5g**).

As suggested by modelling, the 16-membered macrocycle obtained with the Lys side chain was optimal. The 15-membered macrocycle Orn peptide **5b**, on the other hand, had much diminished potency and was only marginally more active than the unconstrained linear reference peptide **6**. The 14- and 13-membered macrocycle peptides obtained by incorporation of A_2bu (**5c**) and A_2pr (**5d**) were essentially devoid of inhibitory activity.

Two of the main objectives in the design of peptidomimetic cyclin groove inhibitors are the minimisation of both molecular mass and overall charge of the peptide leads. We have partly achieved this in the linear $p21^{WAF1}$-derived peptide series, where *e.g.* the pentapeptide H-Arg-Arg-Leu-Ile-(*p*-F-Phe)-NH_2 retains low micromolar potency. The overall charge on the peptide is still high, however, and we therefore investigated *N*-terminal truncation of the optimal cyclic peptide **5a**. We found that whereas truncation of the linear peptide **6** abolished activity completely, truncation of three residues was tolerated, the cyclic pentapeptide **5f** (Table 1) retaining appreciable activity. This result is underlined by the results for the equivalent open chain pentamer structure (**9**), which is effectively devoid of activity.

NMR structural analysis of cyclic peptides

As mentioned above, cyclisation of some peptides resulted in formation of two isomers. In order to unambiguously assign the head- and side chain-to-tail isomers, a 2-D NMR analysis was performed. After assignment of ^1H resonances, the side chain correlations were examined by 2-D TOCSY NMR. The spectra

Table 2 Chemical shift assignments for backbone and sidechain amide protons for **5a** and **5c**

Cyclo **5**–**8** AAUR(Dap)LFG			Cyclo **5**–**8** AAURKLFG		
Residue	NH	CH	Residue	NH	CH
Ala	—	—	Ala	8.16	4.32
Ala	8.39	4.37	Ala	8.17	4.26
Abu	8.19	4.22	Abu	7.93	4.19
Arg	8.33	4.34	Arg	8.08	4.35
Dap	8.21, 7.09 (β NH)	4.53	Lys	8.00, 7.52 (δ NH)	4.38
Leu	8.52	4.23	Leu	8.38	4.31
Phe	8.47	4.49	Phe	8.30	4.32
Gly	8.06	4.25, 3.61	Gly	8.53	4.11, 3.63

obtained for the desired side chain-to-tail cyclic peptides indicated the presence of through-bond connections between the diamino acid residue α-amide and side-chain amide protons (Fig. 2). In addition, through-space connections (2-D NOESY) were observed between the diamino acid and Gly residues, giving additional evidence. The similar constraint in **5a** was also confirmed by NMR (Table 2).

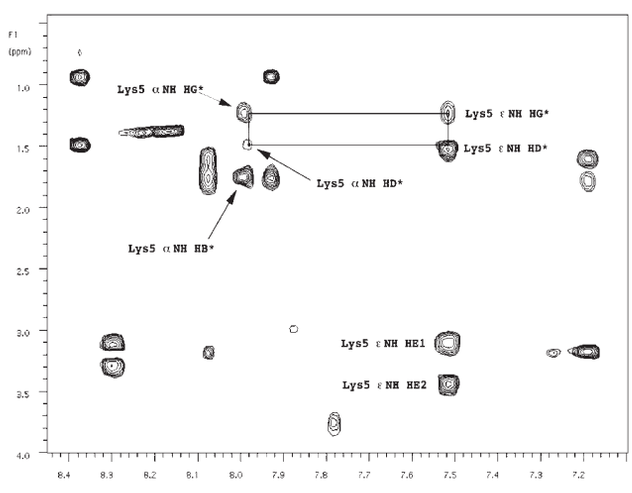

Fig. 2 Correlations from the TOCSY spectrum of the AAURKLFG cyclic peptide, **5c**. The labelled cross-peaks for lysine in position 5 confirm the presence of the side chain to tail cyclic constraint.

Comparisons of the ^{1}H resonances for the inactive A_2bu peptide **5c** suggested that this restrained structure occupies a significantly different conformational space to that of the highly potent Lys derivative **5a** (Table 2). This is primarily shown by the shifts of 0.4 and 0.5 ppm respectively, for the sidechain amides of position 5 and the **5c** Gly NH compared to **5a**. Additionally Phe αCH in **5c** underwent a shift of 0.2 ppm relative to that in **5a.** As this Phe residue is the most critical residue for cyclin A binding and as its conformation is obviously perturbed in this example, a clear rationale for the decrease in potency can be seen.

These NMR results are directly in line with the data obtained from the MD simulations mentioned previously. Both confirm that there are significant differences in the conformational preferences of the two molecules and that this is reflected in their differential binding and inhibition of CDK2A kinase activity. Fig. 3 demonstrates that a correlation between rmsd (from the p27 bound structure for the different ring sizes) and peptide potency is observed indicating that the closest structure to the bound conformation is the most active.

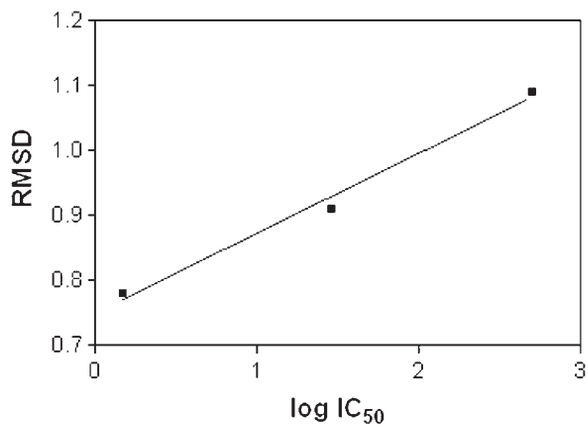

Fig. 3 Plot of the rmsd of the cyclic peptide structure from that of the corresponding region in native p27/cyclin Abound structure. A linear correlation between proximity to the linear structure and the log IC_{50} is observed.

X-Ray crystallography

The CDK2A/peptide **5f** complex structure was solved using a novel crystal form detailed elsewhere.[22] The crystal has space group $P2_12_12_1$ and contains two copies of the binary protein complex in the crystallographic asymmetric unit. One CBG in this complex is fully exposed to the solvent, whilst the other is partially occluded by a CDK2 molecule from a neighbouring crystallographic unit.

The differences between the bound cyclic peptides in the two CBGs are illustrated in Fig. 4a. The RMS deviation for all atoms (46) after superposition was 0.65 Å. In both cases Arg, Leu, and Phe make similar contacts, with some variation in the Lys side chain-to-Gly tail amide and the *C*-terminus. The macrocyclic lactam does not form any contacts with the CBG, and in fact extends out of the groove (Fig. 4b) by up to 13 Å. As a result, the peptides bound to the free and partially occluded CBGs make contacts with the T-loop and the Gly-rich loop (residue 12–18) of neighbouring CDK2 molecules, respectively. The small differences between the two copies of the peptide are probably a result of these contacts.

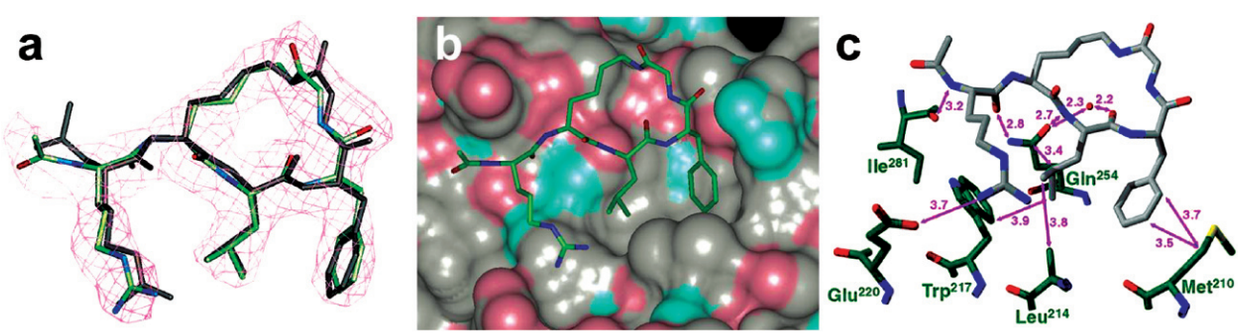

Fig. 4 (a) Superimposition of the structures of peptide **5f** in the free (CPK colouring) and partially occluded (black) cyclin A binding groove present in the asymmetric crystallographic unit of the CDK2A-peptide complex; the 2*Fo*–1*Fc* electron density map is contoured at a level corresponding to 1.2σ for the peptides bound to the non-occluded site. (b) Peptide **5f** bound in the cyclin groove (CPK surface). (c) Main interactions of peptide **5f** (grey C) with residues of the CBG (green C); interatomic distances <4 Å are indicated.

The CBG consists primarily of the cyclin A α1, α3, and α4 helices, and the residues making specific contacts with the ligand peptides include Met^{210}, Ile^{213}, Leu^{214}, Trp^{217}, Glu^{220}, Leu^{253}, Gln^{254}, Ile^{281}, and Thr^{285} (Fig. 4c). In our peptide complex structures, most residues in the CBG are rigid, and their average *B* factors do not change upon ligand binding.

Crystallographic and computational studies help to rationalize the differences in affinity and potency of unconstrained peptides containing either the Leu-Ile-Phe or Leu-Phe-Gly CRM sub-motifs (Fig. 5). Firstly, the energetic cost of binding for the Leu-Phe-Gly segment in unconstrained form is comparatively high, since its bound conformation is not favoured in solution. Secondly, a water-bridged H-bond between the Leu carbonyl and the Gln^{254} side chain is only observed in complex structures of Leu-Ile-Phe containing peptide ligands.[22] This H-bond is lost with the unconstrained Leu-Phe-Gly sub-motif, as the Leu carbonyl points in the opposite direction. Surprisingly, the Leu carbonyl in the cyclic peptide **5f** structure adopts the H-bonding conformation (Fig. 5), resulting in a water-bridged H-bond between the Leu carbonyl and the Gln^{254} side chain (Fig. 4c). Comparison of the bound positions of the Leu and Phe side chains in the cyclic peptide with those from other peptides shows that in each case these residues occupy a similar volume of the hydrophobic pocket in the CBG.

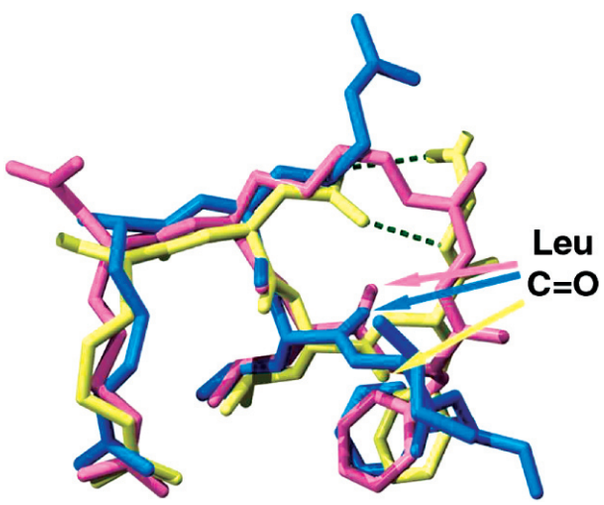

Fig. 5 Superimposition of the cyclin A-bound peptides **5f** (pink), H-Arg-Arg-Leu-Ile-Phe-NH_2 (blue), and the corresponding p27^{KIP1} peptide segment ^{30}Arg-Asn-Leu-Phe-Gly^{34} (yellow).

Computational analysis

In an attempt to better understand the observed differences in affinity between the open chain RNLFG *versus* the AcRKLFG cyclic peptide, intermolecular non-bonded energetics were calculated using the X-ray complex structures of CDK2A/p27 (1JSU) and CDK2A/**5f**. Intramolecular interactions were taken into account in the calculation, and additionally the contribution to binding from the surrounding solvent-mediated H-bonds. Specifically, energetic analysis suggests that a water-mediated H-bond from the Leu^{3} carbonyl to the Gln^{254} side chain provides 10 kcal mol^{-1} to the binding energy of the **5f** cyclic peptide.

The calculations predict that RNLFG (−249 kcal mol^{-1}) binding should be slightly energetically favourable over **5f** (−215 kcal mol^{-1}), even when solvent contributions (−10.7 kcal mol^{-1}) and intramolecular energies are taken into account. This contradicts the established biological assay data, which show the greater potency of **5f** over RNLFG. RNLFG in the bound conformation forms two intramolecular hydrogen bonds (Fig. 4) that hold the peptide in the required conformation and significantly decrease its intramolecular energy. However, it is unlikely that a significant population of intramolecularly H-bonded peptide would exist in solution and RNLFG would adopt a number of different conformations. In the **5f** case the peptide is held in the bound conformation by covalent bonds. This in turn suggests that the driving force in binding of the cyclic peptide is the lower entropic cost of binding and not enthalpy (binding energetics).

Conclusions

The synthesis of side chain-to-main chain cyclic peptides by the methodology used here, *i.e.* intramolecular nucleophilic cleavage from solid support through attack on an activated sulfonamide linker, has not previously been reported. Although solid-phase peptide chain assembly was straightforward, the cyclisation–cleavage reaction required optimisation in terms of protection strategy and reaction conditions. Incorporation of structural constraints into flexible molecules is an approach often used in medicinal chemistry, and is most effective when 3D-structural information of the receptor-bound bioactive conformation of relevant ligands is available. In the case of cyclin groove inhibitors, several crystal structures with various peptide ligands have been reported,[8,9,22,23] and molecular modelling showed that an intramolecular H-bond system observed in the CDK2A-p27^{KIP1} structure could be mimicked with a formal amide linkage in a series of cyclic peptides. The results obtained for the biological activity of these constrained cyclic peptides are in line with the predictions and confirm that introduction of appropriate conformational rigidity is highly productive in terms of potency. Our results show a decrease in activity as the size of the macrocycle is reduced. Introduction of the cyclic constraint also permitted further reduction of peptide mass through truncation, a necessary step in the peptidomimetic process. The cyclic pentapeptide **5f** was co-crystallized with CDK2A, and the complex structure shows that the cyclic constraint allows excellent van der Waals complementarity between the critical Leu and Phe side chains and the hydrophobic pocket in the CBG, without necessitating unfavourable peptide–peptide interactions. Additionally, constraint has allowed in the p27 context, formation of a H-bond involving a structural water molecule previously observed only in the p21 CRM. These factors, along with pre-organisation of the bound conformation, provide us a structural explanation for the affinity of the cyclic molecules relative to their linear counterparts.

Experimental

Peptide synthesis

Peptide chains were assembled using an ABI 433A peptide synthesizer, employing standard Fmoc protection strategy chemistry. Resin was purchased from Novabiochem, all other peptide synthesis reagents, including amino acids, were purchased from ABI. RP-HPLC was performed using Vydac octadecylsilane columns (analytical, 4.6 × 250 mm; preparative, 25 × 250 mm) with acetonitrile–water gradients.

Resin loading. Fmoc-Gly-OH (0.64 g, 2.16 mmol) and 4-sulfamylbutyrylaminomethylpolystyrene resin (0.50 g, nom. 0.54 mmol) were suspended in DMF (4.25 mL), and DIPEA (0.56 mL, 3.24 mmol) was added. The mixture was stirred for 20 min, cooled to −23 °C and PyBOP (1.13 g, 2.16 mmol) was added. The reaction was allowed to warm to room temperature overnight, filtered, washed thoroughly with DMF, and treated with Ac_2O–CH_2Cl_2 (1 : 1; 10 mL) for 1 h. After this time the resin was filtered, washed with CH_2Cl_2, DMF, and Et_2O, and dried *in vacuo*.

Cleavage–cyclisation. Protected peptidyl resin (0.49 g) was shaken with NMP (4 mL) and treated with iodoacetonitrile (0.37 mL, 5.0 mmol) and DIPEA (0.24 mL, 1.25 mmol) under N_2 for 24 h. After this time, the resin was washed thoroughly, dried, and the Mtt protecting group removed by treatment with 1.5% TFA, 3% MeOH in 1,2-dichloroethane (3 × 5 mL, 5 min each). The resin was washed with 1,2-dichloroethane,

Table 3 Analytical details of peptides

No.	Structure: Seq-*Xaa*-Leu-Phe-Gly — Seq	*Xaa*	Yield (%)[a]	HPLC: R_t/min[b]	HPLC: Purity (%)[c]	Formula	M_r	M + H]$^+$ observed[d]
5a	Ac-Ala-Ala-Abu-Arg	Lys	6.4	15.7	>98	$C_{41}H_{66}N_{12}O_9$	871.06	869.5
5b	Ac-Ala-Ala-Abu-Arg	Orn	1.3	18.6	>98	$C_{40}H_{64}N_{12}O_9$	857.03	856.1
5c	Ac-Ala-Ala-Abu-Arg	A_2bu	0.5	18.8	>98	$C_{39}H_{62}N_{12}O_9$	843.00	841.4
5d	Ac-Ala-Ala-Abu-Arg	A_2pr	3.0	20.9	>98	$C_{38}H_{60}N_{12}O_9$	828.98	826.4
5f	Ac-Arg	Lys	1.5	16.8	>98	$C_{31}H_{49}N_9O_6$	643.79	647.1
5e	Ac-Ser-Ala-Abu-Arg	Lys	3.1	10.4	>80	$C_{41}H_{66}N_{12}O_{10}$	887.06	889.8
5g	H-His-Ala-Lys-Arg	Lys	6.2	14.4	>98	$C_{44}H_{71}N_{15}O_8$	938.14	938.9
5h	H-His-Ala-Lys-Arg	Orn	8.9	14.1	>98	$C_{43}H_{69}N_{15}O_8$	924.11	923.4
5i	H-His-Ala-Lys-Arg	A_2bu	6.7	12.6	>98	$C_{42}H_{67}N_{15}O_8$	910.10	910.8
6	Ac-AlaAlaAbuArgAsnLeuPheGly-NH_2		25	11.1	>98	$C_{42}H_{68}N_{16}O_9$	941.09	942.0

[a] Pure peptide with respect to Fmoc-Gly resin loading. [b] Vydac 218TP54 column, 0–60%MeCN/0.1% aq TFA. [c] By integration of HPLC chromatograms (λ = 215 nm). [d] DE-MALDI-TOF MS (ACH matrix).

followed by 20% DIPEA in CH_2Cl_2, and Et_2O, and drying *in vacuo*. The product resin (100 mg) was then heated under reflux for 14 h in dry 1,4-dioxane (2 mL) with DMAP (10 mg). After cooling, the resin was filtered and washed with DMF (2 × 5 mL, 5 min). The combined filtrate and washings were evaporated, and the residue was treated with 2.5% tri-*n*-isopropylsilane in TFA for 1 h. The crude cyclic peptide product was collected after precipitation in ice-cold Et_2O, and was purified by preparative RP-HPLC (13–23% MeCN in 0.1% aq TFA gradient). Fractions containing pure cyclic peptide were pooled and lyophilised.

Analysis. (Table 3).

Biochemical assays

Competitive binding assay. This assay was performed using half-area black 96-well microtitre plates. To each well were added: 10 μL assay buffer (25 mM HEPES pH 7, 10 mM NaCl, 0.01% Nonidet P-40, 1 mM dithiothreitol), 10 μL test compound solution (in 10% aq DMSO), 10 μL CDK2/cyclin A (*ca.* 0.3 μg/well purified recombinant human kinase complex) in assay buffer, and 37.5 nM fluoresceinyl-Ahx-His-Ala-Lys-Arg-Arg-Leu-Ile-Phe-NH_2 tracer peptide in assay buffer. After incubation with shaking for 1 h at room temperature, fluorescence polarization was read on a Tecan Ultra plate reader fitted with 485 nm/535 nm excitation/emission filters and a dichroic mirror suitable for fluorescein. IC_{50} values were determined with the ActivityBase suite of software (IDBS, Guildford, UK) using an unconstrained four-parameter dose response equation.

Functional kinase assay. Test compounds were added to reactions containing 50 mM HEPES pH 7.4, 20 mM β-glycerophosphate, 5 mM EGTA, 2 mM dithiothreitol, 1 mM $NaVO_3$, and 20 mM $MgCl_2$, GST-pRb(773–928) solution, 2–5 μg of purified recombinant human CDK2/cyclin A, 15 mM $MgCl_2$, and 100 μM ATP spiked with 30–50 kBq per well of [γ-^{32}P]-ATP. Reactions were incubated with shaking for 30 min at 30 °C before placing on ice, followed by an addition of 5 μL/well of glutathione-Sepharose 4B (Amersham Biosciences). Beads were allowed to bind for 30 min at room temperature with shaking, before filtering on Whatman GF/C filterplates. Plates were washed 4 times with 0.2 mL/well of 50 mM HEPES containing 1 mM ATP. Incorporated radioactivity was determined after adding 50 μL/well MicroScint40 (Packard) using a TopCount scintillation counter (Packard Instruments, Pangbourne, Berks, UK). IC_{50}s were determined with the ActivityBase suite of software (IDBS, Guildford, UK) using an unconstrained four-parameter dose response equation.

X-Ray crystallography and structure determination

For the purposes of crystallisation, human recombinant CDK2 and cyclin A2 (fragment encompassing residues 173–432) were produced as described.[22,24] Preparations containing stoichiometric mixtures of CDK2 and cyclin A were used for crystallisation after concentration by ultrafiltration.

Crystals of the CDK2A-peptide **5f** complex were obtained by our recently developed ligand exchange technique[22] using CDK2A-H-Arg-Arg-Leu-Ile-Phe-NH_2 crystals in a solution containing 18% PEG-3,350, 100 mM trisodium citrate, and 1 mM peptide **5f**.

Crystals of about 0.05 × 0.1 × 0.03 mm were mounted in 0.05–0.1 mm cryo-loops (Hampton Research). The crystals were immersed briefly in a cryoprotectant (28% PEG-3,350 and 0.1 M trisodium citrate) and then flash-frozen in liquid nitrogen. Data were collected at the Daresbury (UK) and Grenoble (France) synchrotron facilities. Data processing was carried out using the programs DENZO and SCALEPACK or MOSFLM and SCALA from the CCP4 program suite. The structures were solved by molecular replacement using MOLREP and PDB entries 1HCL or 1CKP as the search model. ARP/wARP was used for initial density interpretation and the addition of water molecules. REFMAC was used for structural refinement. A number of rounds of refinement and model-building with the program Quanta (Accelrys, San Diego, USA) were carried out. Crystallographic data are summarized in Table 4. Coordinates for the CDK2A-peptide **5f** complex have been deposited with the Protein Databank under the accession code 1URC.

Molecular modelling and computational analysis

Cyclic peptides were modelled by modifying the isolated sequence Ser-Ala-Cys-Arg-Asn-Leu-Phe-Gly from the structure coordinates of the CDK2A-p27^{KIP1} complex (PDB accession code 1JSU) using the program InsightII (Accelrys, San Diego, CA). The conformational space available to the A_2pr-, A_2bu-, Orn-, and Lys-cyclic peptides was then simulated using minimization and molecular dynamics routines within the Discover program (CVFF forcefield). The initial minimization step involved 100 steps of BFGS–Newton–Raphson minimization. This was followed by the molecular dynamics phase involving a heating phase with 300 steps at 1 fs per step and an equilibration period with 1000 steps, again at 1 fs per step. Superpositions of molecular dynamics frames and calculations of RMSDs with respect to the p27^{KIP1} crystal structure were performed using InsightII. Energetic calculations were carried out using the Discover and Docking modules in InsightII.

Table 4 Crystallographic data for the CDK2A-peptide **5f** complex[a]

Data collection		
Space group		$P2_12_12_1$
Unit cell	*a*/Å	74.7
	b/Å	113.5
	c/Å	155.5
Max. resolution/Å		2.6
Observations		113421
Unique reflections		46681
Completeness (%)		98.9
R_{merge}		0.11
Mean I/σ		5.3
Highest resolution bin		2.74–2.6
Mean I/σ (highest resolution bin)		1.0
R_{merge} (highest resolution bin)		0.52

[a] Refer to Table 1 and Fig. 2.

Refinement	
Protein atoms	8924
Inhibitor atoms	92
Water molecules	339
Reflections used in refinement	39372
R_{factor}	17.5
R_{free}	25.5
Mean *B*-factor, protein/Å^2	45.6
Mean *B*-factor, ligands/Å^2	48.6
Mean *B*-factor, solvent/Å^2	45.1

NMR spectroscopy

Cyclic peptides were dissolved to a concentration of *ca.* 1 mM in a volume of 500 μL of 20 mM aq NaOAc, pH 5, containing 10% D_2O and 0.10 mM sodium 2,2-dimethyl-2-silapentane-5-sulfonate (DSS, internal standard), and the final pH was adjusted to 5.3. ^{1}H, 1-D and 2-D spectra, including TOSCY[25] and NOESY,[26] were acquired at 500 MHz using a Varian Inova spectrometer equipped with a triple resonance probe and a *z* axis pulse field gradient. These experiments were conducted at 298 K and referenced relative to the internal DSS standard. Pulse sequences incorporated the Watergate method for solvent suppression.[27]

References

1 E. Lees, B. Faha, V. Dulic, S. I. Reed and E. Harlow, *Genes Dev.*, 1992, **6**, 1874.
2 A. A. Russo, P. D. Jeffrey and N. P. Pavletich, *Nat. Struct. Biol.*, 1996, **3**, 696.
3 M. Malumbres and M. Barbacid, *Nat. Rev. Cancer*, 2001, **1**, 222.
4 P. M. Fischer, J. Endicott and L. Meijer, *Prog. Cell Cycle Res.*, 2003, **5**, 235.
5 Y.-N. P. Chen, S. K. Sharma, T. M. Ramsey, L. Jiang, M. S. Martin, K. Baker, P. D. Adams, K. W. Bair and W. G. Kaelin, *Proc. Natl. Acad. Sci. USA*, 1999, **96**, 4325.
6 C. McInnes, M. J. I. Andrews, D. I. Zheleva, D. P. Lane and P. M. Fischer, *Curr. Med. Chem. Anti-Cancer Agents*, 2003, **3**, 57.
7 D. Y. Takeda, J. A. Wohlschlegel and A. Dutta, *J. Biol. Chem.*, 2001, **276**, 1993.
8 N. R. Brown, M. E. Noble, J. A. Endicott and L. N. Johnson, *Nat. Cell Biol.*, 1999, **1**, 438.
9 A. A. Russo, P. D. Jeffrey, A. K. Patten, J. Massague and N. P. Pavletich, *Nature*, 1996, **382**, 325.
10 S. K. Sia, P. A. Carr, A. G. Cochran, V. N. Malashkevich and P. S. Kim, *Proc. Natl. Acad. Sci. USA*, 2002, **99**, 14664.
11 P. Li, P. P. Roller and J. Xu, *Curr. Org. Chem.*, 2002, **6**, 411.
12 H. Mihara, S. Yamabe, T. Niidome and H. Aoyagi, *Tetrahedron Lett.*, 1995, **36**, 4837.
13 G. Ösapay and M. Goodman, *J. Chem. Soc., Chem. Commun.*, 1993, 1599.
14 L. Yang and G. Morriello, *Tetrahedron Lett.*, 1999, **40**, 8197.
15 B. J. Backes and J. A. Ellman, *J. Org. Chem.*, 1999, **64**, 2322.
16 D. I. Zheleva, C. McInnes, A.-L. Gavine, N. Z. Zhelev, P. M. Fischer and D. P. Lane, *J. Peptide Res.*, 2002, **60**, 257.
17 G. E. Atkinson, A. Cowan, C. McInnes, D. I. Zheleva, P. M. Fischer and W. C. Chan, *Bioorg. Med. Chem. Lett.*, 2002, **12**, 2501.
18 C. C. Leznoff, *Acc. Chem. Res.*, 1978, **11**, 327.
19 W. C. Chan and P. D. White, in *Fmoc Solid Phase Peptide Synthesis: A Practical Approach*, ed. B. D. Hames, Oxford University Press, Oxford, 2000.
20 A. Aletras, K. Barlos, D. Gatos, S. Koutsogianni and P. Mamkos, *Int. J. Peptide Protein Res.*, 1995, **45**, 488.
21 L. Bourel, O. Carion, H. Gras-Masse and O. Melnyk, *J. Peptide Sci.*, 2000, **6**, 264.
22 G. Kontopidis, M. J. I. Andrews, C. McInnes, A. Cowan, H. Powers, L. Innes, A. Plater, G. Griffiths, D. Paterson, D. I. Zheleva, D. P. Lane, S. Green, M. D. Walkinshaw and P. M. Fischer, *Structure*, 2003, in press.
23 E. D. Lowe, I. Tews, K. Y. Cheng, N. R. Brown, S. Gul, M. E. M. Noble, S. J. Gamblin and L. N. Johnson, *Biochemistry*, 2002, **41**, 15625.
24 S. Y. Wu, I. McNae, G. Kontopidis, S. J. McClue, C. McInnes, K. J. Stewart, S. Wang, D. I. Zheleva, H. Marriage, D. P. Lane, P. Taylor, P. M. Fischer and M. D. Walkinshaw, *Structure*, 2003, **11**, 399.
25 A. Bax, *Bull. Magn. Reson.*, 1985, **7**, 167.
26 J. Jeener, B. H. Meier, P. Bachmann and R. R. Ernst, *J. Chem. Phys.*, 1979, **71**, 4546.
27 M. Piotto, V. Saudek and V. Sklenar, *J. Biomol. NMR*, 1992, **2**, 661.